Certified Rapid Solution of Parametrized Linear Elliptic Equations: Application to Parameter Estimation

N. C. Nguyen*, G. R. Liu*†, A. T. Patera *‡
*Singapore-MIT Alliance
†Department of Mechanical Engineering, National University of Singapore
‡Department of Mechanical Engineering, Massachusetts Institute of Technology

***Abstract*— We present a technique for the rapid and reliable evaluation of linear-functional output of elliptic partial differential equations with affine parameter dependence. The essential components are (*i*) rapidly uniformly convergent reduced-basis approximations — Galerkin projection onto a space W_N spanned by solutions of the governing partial differential equation at N (optimally) selected points in parameter space; (*ii*) *a posteriori* error estimation — relaxations of the residual equation that provide inexpensive yet sharp and rigorous bounds for the error in the outputs; and (*iii*) offline/online computational procedures — stratagems that exploit affine parameter dependence to decouple the generation and projection stages of the approximation process. The operation count for the online stage — in which, given a new parameter value, we calculate the output and associated error bound — depends only on N (typically small) and the parametric complexity of the problem. The method is thus ideally suited to the many-query and real-time contexts.**
In this paper, based on the technique we develop a robust inverse computational method for very fast solution of inverse problems characterized by parametrized partial differential equations. The essential ideas are in three-fold: first, we apply the technique to the forward problem for the rapid certified evaluation of PDE input-output relations and associated rigorous error bounds; second, we incorporate the reduced-basis approximation and error bounds into the inverse problem formulation; and third, rather than regularize the goodness-of-fit objective, we may instead identify all (or almost all, in the probabilistic sense) system configurations consistent with the available experimental data — well-posedness is reflected in a bounded "possibility region" that furthermore shrinks as the experimental error is decreased.

Keywords: Linear elliptic equations, Reduced-basis method, Reduced-basis approximation, *A posteriori* error estimation, Parameter estimation, Inverse computational method, Possibility region.

I. Introduction

Engineering analysis requires the prediction of (say, a single) selected "output" $s^{\rm e}$ relevant to ultimate component and system performance[1]: typical outputs include energies and forces, critical stresses or strains, flowrates or pressure drops, and various local and global measures of concentration, temperature, and flux. These outputs are functions of system parameters, or "inputs," μ, that serve to identify a particular realization or configuration of the component or system: these inputs typically reflect geometry, properties, and boundary conditions and loads; we shall assume that μ is a P-vector (or P-tuple) of parameters in a prescribed closed input domain $\mathcal{D} \subset \mathbb{R}^P$. The input-output relationship $s^{\rm e}(\mu)\colon \mathcal{D} \to \mathbb{R}$ thus encapsulates the behavior relevant to the desired engineering context.

In many important cases, the input-output function $s^{\rm e}(\mu)$ is best articulated as a (say) linear functional ℓ of a field variable $u^{\rm e}(\mu)$. The field variable, in turn, satisfies a μ-parametrized partial differential equation (PDE) that describes the underlying physics: for given $\mu \in \mathcal{D}$, $u^{\rm e}(\mu) \in X^{\rm e}$ is the solution of

$$a(u^{\rm e}(\mu), v; \mu) = f(v), \quad \forall\ v \in X^{\rm e}, \tag{1}$$

where $a(\cdot, \cdot; \mu)$ and f are continuous bilinear and linear forms, respectively; and $X^{\rm e}$ is an appropriate Hilbert space defined over the physical domain $\Omega \subset \mathbb{R}^d$. Relevant system behavior is thus described by an implicit "input-output" relationship

$$s^{\rm e}(\mu) = \ell(u^{\rm e}(\mu)). \tag{2}$$

The problem of evaluating input-output relationship, which requires solution of the underlying partial differential equation (1), is called *forward problem*. In contrast, the *inverse problem* is concerned with deducing the inputs from the measured-observable outputs.

Our particular interest — or certainly the best way to motivate our approach — is in specific areas of inverse problems that take real-time aspect as high priority. For example, in nondestructive evaluation, we may be interested in assessment, evolution, and accommodation of a crack in a critical component of an in-service jet engine. Typical computational tasks include robust parameter estimation (inverse problems) and adaptive design (optimization problems): in the former — for example, assessment of current crack length — we must deduce inputs μ representing system characteristics based on outputs $s^{\rm e}(\mu)$ reflecting measured observables; in the latter — for example, prescription of allowable load — we must deduce inputs μ representing "control" variables based on outputs $s^{\rm e}(\mu)$ reflecting current process objectives. Both of these demanding activities must support an *action* in the presence of continually evolving environmental and mission parameters.

[1]Here superscript "e" shall refer to "exact." We shall later introduce a "truth approximation" which will bear no superscript.

The computational requirements on the forward problem are thus formidable: the evaluation must be *real-time*, since the action must be *immediate*; and the evaluation must be *certified* — endowed with a rigorous error bound — since the action must be *safe* and *feasible*. For example, in our aerospace crack example, we must predict *in the field* — without recourse to a lengthy computational investigation — the load that the potentially damaged structure can unambiguously *safely* carry. Classical approaches such as the finite element method can not typically satisfy these requirements. In the finite element method, we first introduce a piecewise-polynomial "truth" approximation subspace X ($\subset X^{\rm e}$) of dimension $\mathcal{N}$. The "truth" finite element approximation is then found by (say) Galerkin projection: given $\mu \in \mathcal{D}$,

$$s(\mu) = \ell(u(\mu)) \tag{3}$$

where $u(\mu) \in X$ satisfies

$$a(u(\mu), v; \mu) = f(v), \quad \forall\ v \in X. \tag{4}$$

We assume — hence the appellation "truth" — that X is sufficiently rich that $u(\mu)$ (respectively, $s(\mu)$) is sufficiently close to $u^{\rm e}(\mu)$ (respectively, $s^{\rm e}(\mu)$) for all μ in the parameter domain $\mathcal{D}$. Unfortunately, for any reasonable error tolerance, the dimension $\mathcal{N}$ needed to satisfy this condition — even with the application of appropriate (parameter-dependent) adaptive mesh refinement strategies — is typically extremely large, and in particular much too large to provide real-time response in the "deployed" context.

We shall make two crucial hypotheses. The first hypothesis is related to well-posedness, and is often verified only *a posteriori*. We assume that a satisfies a stability and continuity condition

$$0 < \beta_0 \le \beta(\mu) \equiv \inf_{w\in X} \sup_{v\in X} \frac{a(w,v;\mu)}{\|w\|_X \|v\|_X},\ \forall \mu \in \mathcal{D}; \tag{5}$$

$$\gamma(\mu) \equiv \sup_{w\in X} \sup_{v\in X} \frac{a(w,v;\mu)}{\|w\|_X \|v\|_X} < \infty,\ \forall \mu \in \mathcal{D}. \tag{6}$$

Here $\beta(\mu)$ is the Babuška "inf–sup" (stability) parameter — the minimum (generalized) singular value associated with our differential operator — and $\gamma(\mu)$ is the standard continuity constant.

The second hypothesis is related primarily to numerical efficiency, and is typically verified *a priori*. We assume that a is *affine* in the parameter μ in the sense that

$$a(w,v;\mu) = \sum_{q=1}^{Q} \Theta^q(\mu) a^q(w,v), \tag{7}$$

for $q = 1, \ldots, Q$ parameter-*dependent* functions $\Theta^q(\mu) : \mathcal{D} \to \mathbb{R}$ and parameter-*independent* continuous blinear forms $a^q(w,v)$. The affine assumption may in fact be relaxed [3].

II. Reduced-Basis Approximation

The reduced-basis (RB) approximation was first introduced in the late 1970s in the context of nonlinear structural analysis [1], [15] and subsequently abstracted and analyzed [4], [17], [20] and extended [9], [10], [16] to a much larger class of parametrized partial differential equations. We first introduce nested samples $S_N \equiv \{\mu_1 \in \mathcal{D}, \ldots, \mu_N \in \mathcal{D}\}$, $1 \le N \le N_{\rm max}$, and associated nested "Lagrangian" RB spaces $W_N \equiv \text{span}\,\{\zeta_n(\mu_n) \equiv u(\mu_n), 1 \le n \le N\}$, $1 \le N \le N_{\rm max}$.[2] Our RB approximation is then: Given $\mu \in \mathcal{D}$, we evaluate

$$s_N(\mu) = \ell(u_N(\mu))\ , \tag{8}$$

where $u_N(\mu) \in W_N$ satisfies

$$a(u_N(\mu), v; \mu) = f(v),\ \forall\, v \in W_N. \tag{9}$$

We consider in this paper only Galerkin projection, though Petrov-Galerkin approaches can be advantageous. We note that the RB approximation is constructed not as an approximation to the exact solution, $u^{\rm e}(\mu)$, but rather as an approximation to the (finite element) truth approximation, $u(\mu)$. As already discussed, $\mathcal{N}$, the dimension of X, will be very large; our RB formulation and associated error estimation procedures must be *stable* and (online) *efficient* as $\mathcal{N} \to \infty$.

In essence, W_N comprises "snapshots" on the parametrically induced manifold $\mathcal{M} \equiv \{u(\mu) \,|\, \mu \in \mathcal{D}\} \subset X$. It is clear that $\mathcal{M}$ is very *low-dimensional*; furthermore, it can be shown — we consider the equations for the sensitivity derivatives and invoke stability and continuity — that $\mathcal{M}$ is very *smooth*. We thus anticipate that $u_N(\mu) \to u(\mu)$ very rapidly, and that we may hence choose $N \ll \mathcal{N}$. Many numerical examples justify this expectation [8]; and, in certain simple cases, exponential convergence can be proven [12], [19]. We emphasize that the deployed context requires global reduced-basis approximations that are *uniformly* (rapidly) convergent over the entire parameter domain $\mathcal{D}$; proper choice of the parameter samples S_N is thus crucial.

We may now represent $u_N(\mu)$ as $u_N(\mu) = \sum_{j=1}^{N} u_{N\,j}$. Our RB output may then be expressed as $s_N(\mu) = \sum_{j=1}^{N} u_{N\,j}(\mu)\ell(\zeta_j)$, where — we now invoke our affine assumption (7) — the $u_{N\,j}(\mu), 1 \le j \le N$, satisfy the $N \times N$ linear algebraic system

$$\sum_{j=1}^{N} \Big\{ \sum_{q=1}^{Q} \Theta^q(\mu) a^q(\zeta_j, \zeta_i) \Big\} u_{N\,j}(\mu) = f(\zeta_i), \tag{10}$$

for $i = 1, \ldots, N$. It is clear from (10) that we may pursue an offline-online computational strategy [2], [10], [19] that is ideally suited to the deployed real-time context.

In the *offline* stage — performed *once* — we first solve for the ζ_i, $1 \le i \le N_{\rm max}$; we then form *and store* $\ell(\zeta_i), 1 \le i \le N_{\rm max}$, and $a^q(\zeta_j, \zeta_i),\ 1 \le i, j \le N_{\rm max},\ 1 \le q \le Q$. In the

[2] In actual practice, the bases should be orthogonalized with respect to the inner product associated with the Hilbert space X, $(\cdot,\cdot)_X$; the algebraic systems then inherit the "conditioning" properties of the underlying partial differential equation.

online stage — performed many times, for each new μ "in the field" — we first assemble and subsequently invert the (full) $N \times N$ "stiffness" matrix $\sum_{q=1}^{Q} \Theta^q(\mu) a^q(\zeta_j, \zeta_i)$ to obtain the $u_{N\,j}$, $1 \le j \le N$ — at cost $O(QN^2) + O(N^3)$; we then evaluate the sum $\sum_{j=1}^{N} u_{N\,j}(\mu)\ell(\zeta_j)$ to obtain $s_N(\mu)$ — at cost $O(N)$. The online complexity is *independent* of $\mathcal{N}$, and hence — given that $N \ll \mathcal{N}$ — we shall realize extremely rapid deployed response.

III. A Posteriori Error Estimation

We assume for now that we are given $\tilde{\beta}(\mu)$, a (to-be-constructed) positive lower bound for the inf-sup parameter, $\beta(\mu)$: $\beta(\mu) \ge \tilde{\beta}(\mu) \ge \tilde{\beta}_0 > 0$, $\forall \mu \in \mathcal{D}$. We then introduce the dual norm of the residual: $\varepsilon_N(\mu) \equiv \sup_{v \in X} [R(v;\mu)/\|v\|_X]$, where $R(v;\mu) \equiv f(v) - a(u_N(\mu), v; \mu)$ is the residual associated with $u_N(\mu)$. We may now define our "energy" error estimator

$$\Delta_N(\mu) \equiv \frac{\varepsilon_N(\mu)}{\tilde{\beta}(\mu)} \ , \tag{11}$$

and associated effectivity as

$$\eta_N(\mu) \equiv \frac{\Delta_N(\mu)}{\|u(\mu) - u_N(\mu)\|_X} \ . \tag{12}$$

We can then readily demonstrate [19], [22] that for any N, $1 \le N \le N_{\max}$,

$$1 \le \eta_N(\mu) \le \gamma(\mu)/\tilde{\beta}(\mu), \quad \forall\, \mu \in \mathcal{D} \ . \tag{13}$$

The left inequality states that $\Delta_N(\mu)$ is a rigorous upper bound for $\|u(\mu) - u_N(\mu)\|_X$; the right inequality states that $\Delta_N(\mu)$ is a (reasonably) sharp upper bound for $\|u(\mu) - u_N(\mu)\|_X$. We further define an error bound for the output

$$\Delta_N^s(\mu) \equiv \sup_{v \in X} \frac{\ell(v)}{\|v\|_X} \Delta_N(\mu) \ ; \tag{14}$$

for which we clearly obtain

$$|s(\mu) - s_N(\mu)| \le \Delta_N^s(\mu), \ \forall\, \mu \in \mathcal{D} \ . \tag{15}$$

It remains to develop appropriate constructions and associated offline-online computational procedures for the efficient calculation of $\varepsilon_N(\mu)$ and $\tilde{\beta}(\mu)$. We consider the former [14], [19]. To begin, we note from standard duality arguments that

$$\varepsilon_N(\mu) \equiv \sup_{v \in X} \frac{R(v;\mu)}{\|v\|_X} = \|\hat{e}(\mu)\|_X \ , \tag{16}$$

where $\hat{e}(\mu) \in X$ satisfies

$$(\hat{e}(\mu), v)_X = R(v;\mu), \quad \forall\, v \in X \ . \tag{17}$$

We next observe from our reduced-basis expansion and affine assumption (7) that $R(v;\mu)$ may be expressed as

$$R(v;\mu) = f(v) - \sum_{q=1}^{Q} \sum_{n=1}^{N} \Theta^q(\mu) u_{N\,n}(\mu)\, a^q(\zeta_n, v). \tag{18}$$

It thus follows from (17), (18), and linear superposition that

$$\hat{e}(\mu) = \mathcal{C} + \sum_{q=1}^{Q} \sum_{n=1}^{N} \Theta^q(\mu)\, u_{N\,n}(\mu)\, \mathcal{L}_n^q \ , \tag{19}$$

where $\mathcal{C} \in X$ and $\mathcal{L}_n^q \in X$, $1 \le n \le N$, $1 \le q \le Q$ satisfy the *parameter-independent* Poisson(-like) problems $(\mathcal{C}, v) = f(v)$, $\forall\, v \in X$ and $(\mathcal{L}_n^q, v) = -a^q(\zeta_n, v)$, $\forall\, v \in X$, respectively. We then insert the expression (19) into (16) to obtain

$$\begin{aligned} \varepsilon_N^2(\mu) \quad = \quad & (\mathcal{C}, \mathcal{C})_X + \sum_{q=1}^{Q} \sum_{n=1}^{N} \Theta^q(\mu)\, u_{N\,n}(\mu) \Big\{ 2(\mathcal{C}, \mathcal{L}_n^q)_X \\ & + \sum_{q'=1}^{Q} \sum_{n'=1}^{N} \Theta^{q'}(\mu)\, u_{N\,n'}(\mu)\, (\mathcal{L}_n^q, \mathcal{L}_{n'}^{q'})_X \Big\} \ . \end{aligned}$$

An efficient offline-online decomposition may now be identified. In the offline stage — performed once — we first solve for $\mathcal{C}$ and $\mathcal{L}_n^q$, $1 \le n \le N$, $1 \le q \le Q$; we then evaluate and save the relevant parameter-independent inner products $(\mathcal{C}, \mathcal{C})_X$, $(\mathcal{C}, \mathcal{L}_n^q)_X$, $(\mathcal{L}_n^q, \mathcal{L}_{n'}^{q'})_X$, $1 \le n, n' \le N$, $1 \le q, q' \le Q$. Note that all quantities computed in the offline stage are independent of the parameter μ. In the online stage — performed many times, for each new value of μ "in the field" — we simply evaluate $\varepsilon_N^2(\mu)$ in terms of the $\Theta^q(\mu), u_{N\,n}(\mu)$ and the precalculated and stored (parameter-independent) $(\cdot,\cdot)_X$ inner products. The operation count for the online stage is only $O(Q^2N^2)$. Again, the online complexity is *independent of* $\mathcal{N}$ and — for Q not too large — commensurate with the online cost to evaluate $s_N(\mu)$.

Finally, we turn to the development of our lower bound $\tilde{\beta}(\mu)$ for the inf-sup "constant" $\beta(\mu)$. To begin, we note that

$$\beta(\mu) \equiv \sqrt{\inf_{v \in X} \frac{(T^\mu v, T^\mu v)_X}{\|v\|_X^2}} \ , \tag{20}$$

where $T^\mu : X \to X$ is defined as

$$(T^\mu w, v)_X = a(w, v; \mu), \quad \forall\, v \in X. \tag{21}$$

Next given $\overline{\mu} \in \mathcal{D}$ and $t = (t_{(1)} \cdots t_{(P)}) \in \mathbb{R}^P$ — note $t_{(j)}$ is the value of the j^{th} component of t — we introduce the bilinear form

$$\begin{aligned} \mathcal{T}(w, v; t; \overline{\mu}) \quad = \quad & (T^{\overline{\mu}} w, T^{\overline{\mu}} v)_X + \sum_{p=1}^{P} t_{(p)} \Big\{ \sum_{q=1}^{Q} \frac{\partial \Theta^q}{\partial \mu_{(p)}}(\overline{\mu}) \\ & \big[a^q(w, T^{\overline{\mu}} v) + a^q(v, T^{\overline{\mu}} w) \big] \Big\} \end{aligned} \tag{22}$$

and associated Rayleigh quotient

$$\mathcal{F}(t; \overline{\mu}) = \min_{v \in X} \frac{\mathcal{T}(v, v; t; \overline{\mu})}{\|v\|_X^2} \ ; \tag{23}$$

it is readily demonstrated that $\mathcal{F}(t; \bar{\mu})$ is concave in t [13], and hence $\mathcal{D}^{\bar{\mu}} \equiv \{\mu \in \mathbb{R}^P \,|\, \mathcal{F}(\mu - \bar{\mu}; \bar{\mu}) \ge 0\}$ is perforce convex. We next introduce semi-norms $|\cdot|_q \colon X \to \mathbb{R}_{+,0}$ such that

$$|a^q(w, v)| \le \Gamma^q\, |w|_q\, |v|_q \ , \quad \forall\, w, v \in X, \ 1 \le q \le Q \ ,$$

$$C_X = \sup_{w \in X} \frac{\sum_{q=1}^{Q} |w|_q^2}{\|w\|_X} \ , \tag{24}$$

for positive parameter-independent constants Γ^q, $1 \le q \le Q$, and C_X. (Note that C_X is typically *independent of* Q, since

the a^q are often associated with non-overlapping subdomains of Ω.) We may then define

$$\Phi(\mu;\overline{\mu}) \equiv C_X \max_{q\in\{1,\ldots,Q\}} \left\{ \Gamma^q \left\| \Theta^q(\mu) - \Theta^q(\overline{\mu}) - \sum_{p=1}^{P} (\mu-\overline{\mu})_{(p)} \frac{\partial \Theta^q}{\partial \mu_{(p)}}(\overline{\mu}) \right\| \right\} \quad (25)$$

for $\mu \equiv (\mu_{(1)} \cdots \mu_{(P)}) \in \mathbb{R}^P$. We now introduce points $\bar{\mu}_j$ and associated polytopes $\mathcal{P}^{\bar{\mu}_j} \subset \mathcal{D}^{\bar{\mu}_j}$, $1 \le j \le J$, such that

$$\mathcal{D} \subset \bigcup_{j=1}^{J} \mathcal{P}^{\bar{\mu}_j} \ , \quad (26)$$

$$\min_{\nu\in\mathcal{V}^{\bar{\mu}_j}} \sqrt{\mathcal{F}(\nu-\bar{\mu}_j;\bar{\mu}_j)} - \max_{\mu\in\mathcal{P}^{\bar{\mu}_j}} \Phi(\mu;\bar{\mu}_j) \ge \epsilon_\beta \beta(\bar{\mu}^j) \quad (27)$$

for $1 \le j \le J$. Here $\mathcal{V}^{\bar{\mu}_j}$ is the set of vertices associated with the polytope $\mathcal{P}^{\bar{\mu}_j}$ — for example, $\mathcal{P}^{\bar{\mu}_j}$ may be a simplex with $|\mathcal{V}^{\bar{\mu}_j}| = P+1$ vertices; and $\epsilon_\beta \in]0,1[$ is a prescribed accuracy constant. Finally, our lower bound is given by

$$\tilde{\beta}(\mu) = \max_{j\in\{1,\ldots,J\} \,|\, \mu\in\mathcal{P}^{\bar{\mu}_j}} \epsilon_\beta \beta(\bar{\mu}_j) \ . \quad (28)$$

It can be readily demonstrated that $\tilde{\beta}(\mu)$ has the requisite theoretical and computational attributes: $\beta(\mu) \ge \tilde{\beta}(\mu) \ge \overline{\epsilon}\,\beta_0 > 0$, $\forall \mu \in \mathcal{D}$, which thus ensures well-posed and rigorous error bounds.

We now turn to the offline/online decomposition. The *offline* stage comprises two parts: the *generation* of a set of points and polytopes/vertices, $\bar{\mu}_j$ and $\mathcal{P}^{\bar{\mu}_j}$, $\mathcal{V}^{\bar{\mu}_j}$, $1 \le j \le J$; and the *verification* that (26) (trivial) and (27) (nontrivial) are indeed satisfied. We focus on verification; generation — quite involved — is described in detail in [13]. To verify (27), the essential observation is that the expensive terms — "truth" eigenproblems associated with β, (20) and $\mathcal{F}$, (23) — are limited to a finite set of *vertices*,

$$J + \sum_{j=1}^{J} |\mathcal{V}^{\bar{\mu}_j}|$$

in total; only for the extremely inexpensive — and typically algebraically very simple — $\Phi(\mu;\bar{\mu}_j)$ terms must we consider minimization over the *polytopes*. The *online* stage (28) is very simple: a search/look-up table, with complexity logarithmic in J and polynomial in P.

In conclusion, we can calculate a rigorous and sharp upper bound $\Delta_N^s(\mu) = \varepsilon_N^2(\mu)/\tilde{\beta}(\mu)$ for $|s(\mu) - s_N(\mu)|$ with online complexity *independent* of $\mathcal{N}$. These inexpensive error bounds serve most crucially in the online stage — to choose optimal N, to confirm the desired accuracy, to establish strict feasibility, and to control sub-optimality. However, the bounds may also be gainfully enlisted in the offline stage — to construct optimal samples S_N: Given $S_1^{\rm opt} = \mu_1^*$ [DO $N = 2, ..., N_{\max}$; $S_N^{\rm opt} = S_{N-1}^{\rm opt} \cup \mu_N^*$; $\mu_N^* = \arg\max_{\mu\in\Xi^F} \Delta_{N-1}^s(\mu)$; END]; our input sample Ξ^F can be very large since the marginal cost to evaluate $\Delta_N^s(\mu)$ is very small.[3]

[3] In contrast to standard POD economization procedures [21] *we never form the rejected snapshots*: our inexpensive bound $\Delta_N^s(\mu)$ serves as a (good) surrogate for the actual error [14].

IV. A Robust Inverse Computational Method

As mentioned earlier, in inverse problems we are concerned with predicting the unknown parameters from the measured outputs. The inverse problem is of course typically ill-posed. The latter is traditionally addressed by regularization [7]; unfortunately, though adaptive regularization techniques are quite sophisticated, the ultimate prediction is nevertheless affected by the *a priori* assumptions — in ways that are difficult to quantify in a robust fashion.

Our approach promises significant improvements. Thanks to the rapid convergence of the reduced-basis approximation and the offline/online computational stratagem we can, in fact, achieve real-time response in the "deployed" stage; and, thanks to our *a posteriori* error estimators, we can associate rigorous certificates of fidelity to our (very fast) output predictions. These advantages are further leveraged within the inverse-problem context, rather than regularize the goodness-of-fit objective, we may instead identify all (or almost all, in the probabilistic sense) system configurations consistent with the available experimental data. Well-posedness is now reflected in a bounded "possibility region" $\mathcal{R}$ that furthermore shrinks as the experimental error is decreased.

In the context of inverse problems, our input has two components, $\mu = (\nu, \sigma)$, where $\nu \in \mathcal{D}^\nu$ are characteristic-system parameters and σ are experimental control variables. The inverse problems involve determining the true but unknown parameters ν^* from noise-free measurements $\{s(\nu^*, \sigma_k), 1 \le k \le K\}$. In actual practice, due to the presence of noise in measurement our experimental data will be in the form of intervals $\mathcal{I}(\epsilon_{\rm exp}, \sigma_k) \equiv [s(\nu^*,\sigma_k)(1-\epsilon_{\rm exp}), s(\nu^*,\sigma_k)(1+\epsilon_{\rm exp})], k = 1, \ldots, K$, where $\epsilon_{\rm exp}$ is the error in measurement. The inverse problem is then: Given experimental measurements $\mathcal{I}(\epsilon_{\rm exp}, \sigma_k), k = 1, \ldots, K$, we wish to determine the region $\mathcal{P} \in \mathcal{D}^\nu$ in which the unknown parameters ν^* must reside. Towards this end, we define

$$\mathcal{P} \equiv \{\nu \in \mathcal{D}^\nu | s(\nu,\sigma_k) \in \mathcal{I}(\epsilon_{\rm exp}, \sigma_k), 1 \le k \le K\} \quad (29)$$

where $s(\nu,\sigma)$ is determined by (3) and (4). Unfortunately, the realization of $\mathcal{P}$ requires many *queries* of $s(\nu,\sigma)$, which in turn demands repeated solutions of the underlying PDE.

Instead, we shall construct a bounded "possibility region" $\mathcal{R}$ such that $\mathcal{P} \subset \mathcal{R}$. We first apply the reduced-basis method to obtain $s_N^\pm(\mu) \equiv s_N(\mu) \pm \Delta_N^s(\mu)$, and recall that — thanks to our rigorous bounds (15) — $s(\mu) \in [s_N^-(\mu), s_N^+(\mu)]$. We may then define

$$\mathcal{R} \equiv \left\{ \nu \in \mathcal{D}^\nu \,|\, \left[s_N^-(\nu,\sigma_k), s_N^+(\nu,\sigma_k)\right] \cap \mathcal{I}(\epsilon_{\rm exp}, \sigma_k), 1 \le k \le K \right\} \quad (30)$$

clearly, we have accommodated both numerical and experimental error and uncertainty (within our model assumptions), and hence $\nu^* \in \mathcal{P} \subset \mathcal{R}$. The important point is that $\mathcal{R}$ can be constructed very inexpensively since $s_N(\mu)$ and $\Delta_N^s(\mu)$ are computed only in $O(N^3 + Q^2N^2)$ per online evaluation.

Central to our computational inverse method is a robust inverse algorithm to construct $\mathcal{R}$: we first find one point in $\mathcal{R}$; we then conduct a binary chop at different angles to map out the boundary of $\mathcal{R}$. In a future paper, we provide further details and apply the method to more realistic applications.

V. Inverse Scattering Analysis: A Simple Problem

To demonstrate the various aspects of the method and illustrates the contexts in which we develop it, we apply our method to a simple (acoustics) exterior inverse scattering problem. Inverse scattering problems has of course attracted enormous attention due to its practical importance in various areas of engineering and science such as medical, geophysical, defense science. The wide range of applications has stimulated the development of different solution approaches for inverse scattering problems [18], [5], [6]. Our view is that the development of numerical methods in inverse scattering analysis should remain close to the applications and in particular should have the numerical solution in real-time as high priority. However, in almost cases, the techniques are quite expensive — do not accommodate either extensive optimization or real-time response — and do not well quantify uncertainty.

We consider the scattering of a time harmonic acoustic incident wave $u^{\rm inc}(x) = e^{{\rm i}kx^T d}$ moving in direction d by an infinite cylinder with bounded cross section $D^{\rm o}$, where k is the wave number of the incident plane wave $u^{\rm inc}$. Assuming that the object $D^{\rm o}$ is "sound-hard", the scattered wave u satisfies an acoustics exterior Neumann problem

$$\Delta u + k^2 u = 0 \quad \text{in } \mathbb{R}^2 \backslash \overline{D}^{\rm o}, \tag{31a}$$

$$\frac{\partial}{\partial \nu}(u + u^{\rm inc}) = 0 \qquad \text{on } \partial D^{\rm o}, \tag{31b}$$

$$\lim_{r\to\infty} \sqrt{r}\left(\frac{\partial u}{\partial r} - {\rm i}ku\right) = 0, \quad r = |x| \tag{31c}$$

Mathematically, the Sommerfeld radiation condition (31c) ensures the wellposedness of the problem (31); physically it characterizes out-going waves. The scattered wave u has the following asymptotic behavior

$$u(x) = \frac{e^{{\rm i}kr}}{\sqrt{r}} u_\infty(\hat{d}, d) + O\left(\frac{1}{r}\right), \quad \hat{d} = x/|x|, x \to \infty \tag{32}$$

The function u_∞ defined on the unit sphere $S \subset \mathbb{R}^2$ is known as the scattering amplitude or the far-field pattern of the scattered wave. The Green representation theorem and the asymptotic behaviour of the fundamental solution ensures a representation of the far-field pattern in the form [11]

$$u_\infty(\hat{d}) = \kappa \int_{\partial D^{\rm o}} \left\{ u(x) \frac{\partial e^{-{\rm i}k\hat{d}^T x}}{\partial \nu} - \frac{\partial u(x)}{\partial \nu} e^{-{\rm i}k\hat{d}^T x} \right\} \tag{33}$$

where $\kappa = \frac{\rm i}{4}\sqrt{\frac{2}{\pi k}}$ and ν is the normal to the boundary $\partial D^{\rm o}$. Since the problem is posed over indefinite domain, before attempting numerical solutions, it is required to replace the indefinite domain with a artificial closed boundary $\Gamma^{\rm o}$ enclosing the object. A boundary condition is then introduced on $\Gamma^{\rm o}$ in such a way that the resulting boundary-value problem is well-posed and its solution approximates well the restriction of u to the bounded domain $\Omega^{\rm o}$ limited by $\partial D^{\rm o}$ and $\Gamma^{\rm o}$. For the purpose of simplicity, we shall consider simple first-order Sommerfeld radiation condition at large distances, though higher-order approximation may be pursued. Our weak formulation of the exterior Neumann problem is thus: given $\mu \equiv (D^{\rm o}, k, d, \hat{d})$, evaluate $u_\infty(\mu) = \ell(u(\mu); \mu)$, where $u(\mu) \in Z$ is the solution of

$$a(u, v; \mu) = f(v; \mu), \quad \forall v \in Z; \tag{34}$$

here the forms are given by

$$a(w, v; \mu) = \int_{\Omega^{\rm o}} \nabla w . \nabla \bar{v} - k^2 w \bar{v} - {\rm i}k \int_{\Gamma^{\rm o}} w \bar{v}, \tag{35}$$

$$f(v; \mu) = \int_{\partial D^{\rm o}} -{\rm i}k d^T \nu e^{{\rm i}kx^T d} \bar{v}, \tag{36}$$

$$\ell(v; \mu) = \kappa \int_{\partial D^{\rm o}} \left\{ u(x) \frac{\partial e^{-{\rm i}k\hat{d}^T x}}{\partial \nu} - \frac{\partial u(x)}{\partial \nu} e^{-{\rm i}k\hat{d}^T x} \right\}, \tag{37}$$

where Z is the complex function space

$$Z = \{v = v^{\rm R} + {\rm i}v^{\rm I} : v^{\rm R} \in H^1(\Omega^{\rm o}), v^{\rm I} \in H^1(\Omega^{\rm o})\}. \tag{38}$$

Here superscripts R and I denote the real and imaginary part respectively; $\bar{v}$ shall denote the complex conjugate of v, and $|v|$ the modulus of v.

As a simple demonstration we consider an two-dimensional ellipse of unknown major and minor axes (a, b) and unknown orientation α for $D^{\rm o}$. Hence, for given geometric parametrization (a, b, α) and the incident wave $u^{\rm inc}$, the forward problem is to find the scattered wave u and in particular the far field pattern u_∞. In contrast, the inverse problem is to predict the true but unknown parameters (a^*, b^*, α^*) from the knowledge of the far field pattern $u_\infty(k, d, \hat{d}, \epsilon_{exp})$ measured at several directions $\hat{d}$ with experimental error ϵ_{exp} for one or several directions d and wave numbers k. In the language of our notation, the input $\mu \in \mathcal{D} \subset \mathbb{R}^6$ consists of $k, d, \hat{d}, a, b,$ and α in which (a, b, α) are characteristic-system parameters and $(k, d, \hat{d})$ are experimental control variables; and the output $s(\mu)$ is the far-field pattern u_∞. Furthermore, we shall consider the parameter domain $\mathcal{D} \equiv \mathcal{D}^{k,d,\hat{d}} \times \mathcal{D}^{a,b,\alpha}$, where $\mathcal{D}^{k,d,\hat{d}} \equiv [\pi/12, \pi/12] \times [0, 2\pi] \times [0, 2\pi]$ and $\mathcal{D}^{a,b,\alpha} \equiv \times[0.5, 1.5] \times [0.5, 1.5] \times [0, \pi]$ (note here that $a \geq b$ and wave number k is fixed).

We now map $\Omega^{\rm o}(a, b, \alpha)$ via a continuous piecewise-affine transformation to a fixed reference domain Ω.[4] This new problem can now be cast precisely in the desired abstract form (34), in which Ω and Z are independent of the parameter μ. In particular, as required, all parameter dependence now enters through the bilinear form $a(\cdot, \cdot; \mu)$. Furthermore, it is readily demonstrated that our affine assumption (7) applies for

[4]The original domain is bounded by an artificial boundary $\Gamma^{\rm o}$ and the ellipse, where $\Gamma^{\rm o}$ is an oblique rectangle which has the same orientation as the ellipse and is scaled with the minor and major axes of the ellipse. The reference domain is bounded by a square of size $[-5, 5] \times [-5, 5]$ and the boundary of a unit circular reference object.

$Q = 5$. Note however that the force and output functionals f and ℓ are not affine in μ, which implies that our offline-online decomposition may break down. Fortunately, this restriction can be readily addressed by a new empirical interpolation approach in which we replace the nonaffine form with the necessarily affine approximation [3]. On the other side, in general, our *a posteriori* error bounds are no longer completely rigorous, because the empirical interpolation induces a non-rigorous component in the error bounds. We shall articulate the rigorous/nonrigorous facets of the error bounds shortly.

We now present basic numerical results. For the inf-sup lower bound construction, we choose $\bar{\epsilon}_\beta = 0.5$ and thus cover $\mathcal{D}$ such that (26) and (27) are satisfied with only $J = 13$ polytopes[5] (we provide in detail $\Theta^q(\mu)$, $a^q(w, v)$, our choice of $|\cdot|_q$, $1 \leq q \leq 10$, and $(\cdot,\cdot)_X$ in [13]); for our reduced-basis spaces we pursue the optimal sampling strategy described in Section III for $N_{\max} = 62$; we present in Table 1 $\Delta_{N,\max}$, $\eta_{N,\text{ave}}$, $\Delta^s_{N,\max}$, and $\eta^s_{N,\text{ave}}$ as a function of N. Here $\Delta_{N,\max}$ is the maximum over Ξ_{Test} of $\Delta_N(\mu)$, $\eta_{N,\text{ave}}$ is the average over Ξ_{Test} of $\Delta_N(\mu)/\|u(\mu) - u_N(\mu)\|$, $\Delta^s_{N,\max}$ is the maximum over Ξ_{Test} of $\Delta^s_N(\mu)$, and $\eta^s_{N,\text{ave}}$ is the average over Ξ_{Test} of $\Delta^s_N(\mu)/\|s(\mu) - s_N(\mu)\|$, where $\Xi_{\text{Test}} \subset (\mathcal{D})^{343}$ is a random parameter sample of size 256. We observe that the reduced-basis approximation converges very rapidly, and that our rigorous error bounds are in fact quite sharp. The output effectivities are not $O(1)$ primarily due to the relatively crude bounds obtained with the dual norm of the output functional. The adjoint technique can be effectively used to improve the error bounds for the output [19], [14]. However, effectivities $O(10)$ are acceptable within the reduced-basis context: thanks to the very rapid convergence rates, the "unnecessary" increase in N — to achieve a given error tolerance — is proportionately very small.

N	$\Delta_{N,\max}$	$\eta_{N,\text{ave}}$	$\Delta^s_{N,\max}$	$\eta^s_{N,\text{ave}}$
10	3.34×10^{-01}	4.67	2.00×10^{-01}	33.00
20	7.15×10^{-02}	4.15	4.66×10^{-02}	29.75
30	1.54×10^{-02}	5.20	9.41×10^{-03}	25.95
40	6.09×10^{-03}	4.50	3.63×10^{-03}	22.56
50	2.22×10^{-03}	4.86	1.11×10^{-03}	28.26
60	8.27×10^{-04}	4.39	5.02×10^{-04}	31.38

TABLE I: Numerical results for the direct scattering problem.

We next look at the various rigorous and non-rigorous parts of the error bound $\Delta_N(\mu)$. For this purpose, we introduce $\Delta_{N,\text{ave}}$ is the average over Ξ_{Test} of $\Delta_N(\mu)$; $\Delta^{\text{r}}_{N,\text{ave}}$ is the average over Ξ_{Test} of the rigorous part; $\Delta^{\text{n}}_{N,\text{ave}}$ is the average over Ξ_{Test} of the nonrigorous part which is induced by the empirical interpolation (see [13] for a detailed definition of these quantities). We present in Table II these quantities as a function of N. We observe that $\Delta^{\text{r}}_{N,\text{ave}}$ is indeed no different from $\Delta_N(\mu)$, which basically indicates rigor of our error bounds.

[5]The number of polytopes is reasonably small because our bilinear form $a(\cdot,\cdot;\mu)$ in fact depends only on a, b and k, and wave number $k = \pi/12$ is in the low-frequency regime.

N	$\Delta^u_{N,\text{ave}}$	$\Delta^{\text{r}}_{N,\text{ave}}$	$\Delta^{\text{n}}_{N,\text{ave}}$
10	1.80×10^{-01}	1.80×10^{-01}	5.63×10^{-07}
20	3.19×10^{-02}	3.19×10^{-02}	5.63×10^{-07}
30	7.20×10^{-03}	7.20×10^{-03}	5.63×10^{-07}
40	2.38×10^{-03}	2.38×10^{-03}	5.63×10^{-07}
50	1.06×10^{-03}	1.06×10^{-03}	5.63×10^{-07}
60	3.47×10^{-04}	3.46×10^{-04}	5.63×10^{-07}

TABLE II: Rigorous and non-rigorous parts of the error bound as a function of N.

Turning now to computational effort, for (say) $N = 40$ and any given μ (say, $(\pi/12, 0, 0, \pi, 0.5, 0.5)$) — for which the error in the reduced-basis output $s_N(\mu)$ relative to the truth approximation $s(\mu)$ is *certifiably* less than $\Delta^s_N(\mu)$ ($= 4.97 \times 10^{-4}$) — the Online Time (marginal cost) to compute both $s_N(\mu)$ and $\Delta^s_N(\mu)$ is less than 1/126 the Total Time to directly calculate the truth result $s(\mu) = \ell(u(\mu))$. Clearly, the savings will be even larger for problems with more complex geometry and solution structure in particular in three space dimensions. Nevertheless, even for our current very modest example, the computational economies are very significant.

Finally, we consider the characterization of the unknown ellipse — more precisely, the construction of possibility region $\mathcal{R}$ — that illustrates the new capabilities enabled by rapid certified input-output evaluation. In particular, given experimental data in the form of intervals $\mathcal{I}_{exp} \equiv [u_\infty(k, d, \hat{d}, a^*, b^*, \alpha^*)(1 - \epsilon_{\text{exp}}),\ u_\infty(k, d, \hat{d}, a^*, b^*, \alpha^*)(1 + \epsilon_{\text{exp}})]$ measured at several angles $\hat{d}$ with experimental error ϵ_{exp} for several directions d of the incident wave, we seek to identify a region $\mathcal{R} \in \mathcal{D}^{a,b,\alpha}$ in which the true — but unknown — obstacle parameters, a^*, b^* and α^*, must reside. In our numerical experiments, we keep the wave number fixed $k = \pi/12$ and use positive x and positive y directions for the incident wave. For each direction of the incident wave, there are $J(= 4)$ directions $\hat{d}_j, j = 1, \ldots, J$, whose value are given by $\hat{d}_j = 2\pi(j-1)/J, 1 \leq j \leq J$, at which the outputs are collected.

We show in Figures 1a, 1b, and 1c the possibility regions for the major and minor axes and orientiation of our ellipse — more precisely, (more convenient) 3-ellipsoids[6] that *contain* the possibility regions for the minor and major axes and orientation — for experimental error of 5%, 2%, and 1%. As expected, as ϵ_{exp} decreases, $\mathcal{R}$ shrinks toward the exact (synthetic) value, $a^* = 1.25, b^* = 0.75, \alpha^* = 5\pi/8$. More importantly, for any finite ϵ_{exp}, $\mathcal{R}$ *rigorously captures the uncertainty* in our assessment of the obstacle parameters without *a priori* regularization hypotheses [7]. The crucial new ingredient is reliable fast evaluations that permit us to conduct a much more extensive search over parameter space; for a given ϵ_{exp}, $\mathcal{R}$ may be generated online in less than 137 seconds on a Pentium 1.6 GHz thanks to a per forward evaluation time of only 0.028 seconds. Moreover, these pos-

[6]The ellipsoid can be obtained from a set of points representing the possibility region by formulating an appropriate minimization problem that returns the smallest ellipsoid containing the set of points [13].

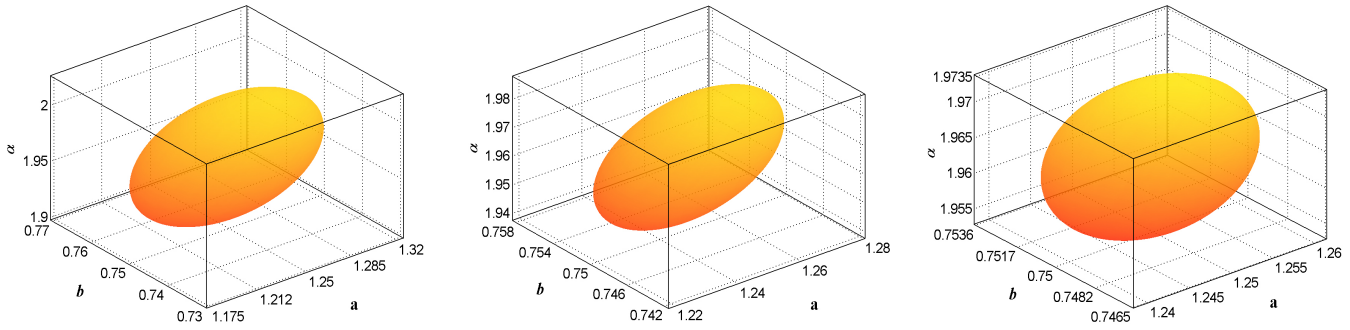

(a) (b) (c)

Fig. 1: Ellipsoids containing possibility regions $\mathcal{R}$ for experimental error of (a) 5%, (b) 2%, and (c) 1%. Note the change in scale in the axes: $\mathcal{R}$ shrinks as the experimental error decreases. The true parameters are $(a^*, b^*) = (1.25, 0.75)$ and $\alpha^* = 5\pi/8$.

sibility regions quantify uncertainty in both the reduced-basis approximation and the inverse-problem assessment; we can thus undertake appropriate real-time actions in the field with some confidence. Of course, our search over possible obstacle parameters will never be truly exhaustive, and hence there may be small undiscovered "pockets of possibility" in $\mathcal{D}^{a,b,\alpha}$; however, we have certainly reduced the uncertainty relative to more conventional approaches. (Needless to say, the procedure can also only *characterize* cracks within our selected low-dimensional parametrization; however, more general null hypotheses can be constructed to *detect* model deviation.)

ACKNOWLEDGEMENTS

We would like to thank Professor Yvon Maday of University Paris VI for his many invaluable contributions to this work. We would also like to thank Dr Karen Veroy of MIT and Mr Martin Grepl of MIT for many helpful recommendations. This work was supported by the Singapore-MIT Alliance.

REFERENCES

[1] B. O. Almroth, P. Stern, and F. A. Brogan. Automatic choice of global shape functions in structural analysis. *AIAA Journal*, 16:525–528, May 1978.

[2] E. Balmes. Parametric families of reduced finite element models: Theory and applications. *Mechanical Systems and Signal Processing*, 10(4):381–394, 1996.

[3] M. Barrault, N. C. Nguyen, Y. Maday, and A. T. Patera. An "empirical interpolation" method: Application to efficient reduced-basis discretization of partial differential equations. *C. R. Acad. Sci. Paris, Série I*, 2004. Submitted.

[4] A. Barrett and G. Reddien. On the reduced basis method. *Z. Angew. Math. Mech.*, 75(7):543–549, 1995.

[5] P. M. Van Den Berg and R. E. Kleinman. Gradient methods in inverse acoustic and electromagnetic scattering. In P.G. Ciarlet and J.L. Lions, editors, *Mathematics and its Applications, Vol. 92*, Large-Scale Optimization with Applications (Part 1), pages 173–194. Springer-Verlag, New York, 1997.

[6] D. Colton, K. Giebermann, and P. Monk. A regularized sampling method for solving three dimensional inverse scattering problems. *SIAM J. Sci. Comput.*, 21:2316–2330, 2000.

[7] H. W. Engl, M. Hanke, and A. Neubauer. *Regularization of Inverse Problems*. Kluwer Academic, Dordrecht, 1996.

[8] M. A. Grepl, N. C. Nguyen, K.Veroy A. T. Patera, and G. R. Liu. Certified rapid solution of parametrized partial differential equations for real-time applications. In *Proceedings of the 2nd Sandia Workshop of PDE-Constrained Optimization: Towards Real-Time and On-Line PDE-Constrained Optimization*, SIAM Computational Science and Engineering Book Series, 2004. submitted for consideration.

[9] M. D. Gunzburger. *Finite Element Methods for Viscous Incompressible Flows: A Guide to Theory, Practice, and Algorithms*. Academic Press, Boston, 1989.

[10] K. Ito and S. S. Ravindran. A reduced-order method for simulation and control of fluid flows. *Journal of Computational Physics*, 143(2):403–425, July 1998.

[11] A. Kirsch. The domain derivative and two applications in inverse scattering theory. *Inverse Problems*, 9:81–96, 1993.

[12] Y. Maday, A. T. Patera, and G. Turinici. Global *a priori* convergence theory for reduced-basis approximation of single-parameter symmetric coercive elliptic partial differential equations. *C. R. Acad. Sci. Paris, Série I*, 335(3):289–294, 2002.

[13] N. C. Nguyen. *Reduced-Basis Approximation and A Posteriori Error Bounds for Nonaffine and Nonlinear Partial Differential Equations: Application to Inverse Analysis*. PhD thesis, Singapore-MIT Alliance, National University of Singapore.

[14] N. C. Nguyen, K. Veroy, and A. T. Patera. Certified real-time solution of parametrized partial differential equations. In *Handbook of Materials Modeling*. Kluwer Academic Publishing, 2004. To appear.

[15] A. K. Noor and J. M. Peters. Reduced basis technique for nonlinear analysis of structures. *AIAA Journal*, 18(4):455–462, April 1980.

[16] J. S. Peterson. The reduced basis method for incompressible viscous flow calculations. *SIAM J. Sci. Stat. Comput.*, 10(4):777–786, July 1989.

[17] T. A. Porsching. Estimation of the error in the reduced basis method solution of nonlinear equations. *Mathematics of Computation*, 45(172):487–496, October 1985.

[18] R. Potthast. A fast new method to solve inverse scattering problems. *Inverse Problems*, 12:731–742, 1996.

[19] C. Prud'homme, D. Rovas, K. Veroy, Y. Maday, A. T. Patera, and G. Turinici. Reliable real-time solution of parametrized partial differential equations: Reduced-basis output bound methods. *Journal of Fluids Engineering*, 124(1):70–80, March 2002.

[20] W. C. Rheinboldt. On the theory and error estimation of the reduced basis method for multi-parameter problems. *Nonlinear Analysis, Theory, Methods and Applications*, 21(11):849–858, 1993.

[21] L. Sirovich. Turbulence and the dynamics of coherent structures, part 1: Coherent structures. *Quarterly of Applied Mathematics*, 45(3):561–571, October 1987.

[22] K. Veroy, C. Prud'homme, D. V. Rovas, and A. T. Patera. *A Posteriori* error bounds for reduced-basis approximation of parametrized noncoercive and nonlinear elliptic partial differential equations (AIAA Paper 2003-3847). In *Proceedings of the 16th AIAA Computational Fluid Dynamics Conference*, June 2003.